Cell

ATAXIN-1 Interacts with the Repressor Capicua in Its Native Complex to Cause SCA1 Neuropathology

Yung C. Lam,[1,9] Aaron B. Bowman,[2,8,9] Paymaan Jafar-Nejad,[2] Janghoo Lim,[2] Ronald Richman,[4] John D. Fryer,[4] Eric D. Hyun,[3] Lisa A. Duvick,[5,6,7] Harry T. Orr,[5,6,7] Juan Botas,[2] and Huda Y. Zoghbi[1,2,3,4,*]
[1] Department of Neuroscience
[2] Department of Molecular and Human Genetics
[3] Program in Developmental Biology
[4] Howard Hughes Medical Institute
Baylor College of Medicine, Houston, TX 77030, USA
[5] Department of Laboratory Medicine and Pathology
[6] Department of Biochemistry
[7] Institute of Human Genetics
University of Minnesota, Minneapolis, MN 55455, USA
[8] Present address: Department of Neurology, Kennedy Center for Research on Human Development, Vanderbilt University, Nashville, TN 37232, USA.
[9] These authors contributed equally to this work.
*Contact: hzoghbi@bcm.tmc.edu
DOI 10.1016/j.cell.2006.11.038

SUMMARY

Spinocerebellar ataxia type 1 (SCA1) is one of several neurodegenerative diseases caused by expansion of a polyglutamine tract in the disease protein, in this case, ATAXIN-1 (ATXN1). A key question in the field is whether neurotoxicity is mediated by aberrant, novel interactions with the expanded protein or whether its wild-type functions are augmented to a deleterious degree. We examined soluble protein complexes from mouse cerebellum and found that the majority of wild-type and expanded ATXN1 assembles into large stable complexes containing the transcriptional repressor Capicua. ATXN1 directly binds Capicua and modulates Capicua repressor activity in *Drosophila* and mammalian cells, and its loss decreases the steady-state level of Capicua. Interestingly, the S776A mutation, which abrogates the neurotoxicity of expanded ATXN1, substantially reduces the association of mutant ATXN1 with Capicua in vivo. These data provide insight into the function of ATXN1 and suggest that SCA1 neuropathology depends on native, not novel, protein interactions.

INTRODUCTION

SCA1 (*Spinocerebellar ataxia type 1*) is one of nine unrelated genes in which expansion of a glutamine-encoding triplet repeat causes a dominantly inherited neurodegenerative disease. Despite broad expression of polyglutamine proteins, distinct subsets of neurons are vulnerable in each disease. Genetic studies have shown that expansion of the polyglutamine tract confers a toxic gain of function (Duyao et al., 1995; Ikeda et al., 2005; Matilla et al., 1998; Matsumoto et al., 2005; Nasir et al., 1995; Zeitlin et al., 1995). The nature of this gain of function has, however, remained mysterious. While it is clear that polyglutamine tract expansion alters the conformation of soluble mutant proteins and decreases protein solubility leading to aggregation (Ross and Poirier, 2004), there is considerable debate as to the biophysical and biochemical state of the disease protein that renders it neurotoxic and the mechanism that leads to selective neuronal vulnerability in each of these disorders.

Emerging data reveal that neurotoxicity is modulated by the context of the polyglutamine expansion. For example, the S776A mutation of polyglutamine-expanded ATAXIN-1 (ATXN1) prevents the ataxia and neurodegeneration caused by expression of the SCA1 disease protein in mouse Purkinje cells (Emamian et al., 2003). Likewise, in Huntington disease, phosphorylation, SUMO modification, or mutation of the Caspase-6 cleavage site modulate the neurotoxicity of mutant Huntingtin (Graham et al., 2006; Luo et al., 2005; Pardo et al., 2006; Rangone et al., 2004; Steffan et al., 2004; Warby et al., 2005). Full-length, but not truncated, polyglutamine-expanded androgen receptor reproduces the sex-specific neuropathology of SBMA (Chevalier-Larsen et al., 2004; Katsuno et al., 2002; McManamny et al., 2002). The discovery that the AXH domain of ATXN1 mediates SCA1 neurotoxicity further emphasized the importance of *cis*-acting

domains in pathogenesis and the relationship between such domains and the polyglutamine tract (Tsuda et al., 2005). Lastly, studies from Huntington and SCA3 models have revealed a genetic interaction between the wild-type proteins and their polyglutamine-expanded counterparts (Cattaneo et al., 2005; Van Raamsdonk et al., 2005; Warrick et al., 2005; Zuccato et al., 2003). These observations suggest a relationship between the selective neurotoxic properties of the polyglutamine-expanded protein and the normal functions of the wild-type protein.

Aberrant protein interactions are thought to mediate neurotoxicity in polyglutamine diseases (Gatchel and Zoghbi, 2005; Harjes and Wanker, 2003; Li and Li, 2004; MacDonald, 2003). Polyglutamine expansion alters the interactions of Huntingtin with HAP1/p150^{Glued}/dynein complexes, as well as numerous transcription factors, leading to their functional impairment (Chen-Plotkin et al., 2006; Dunah et al., 2002; Gauthier et al., 2004; Kegel et al., 2002; Li et al., 2002; Schaffar et al., 2004; Zhai et al., 2005; Zuccato et al., 2003). Other examples of altered protein-protein interactions include Ataxin-7 with CRX and the STAGA/TFTC complexes and Ataxin-3 with components of the ubiquitin proteasome system (Chen et al., 2004; Doss-Pepe et al., 2003; Helmlinger et al., 2006; McMahon et al., 2005; Palhan et al., 2005; Strom et al., 2005; Warrick et al., 2005). Nevertheless, it is unknown if neurotoxicity of the mutant proteins occurs through associations with these native protein complexes, loss of these associations, or aberrant interactions and novel complexes formed by misfolded or aggregating disease protein.

To test the hypothesis that polyglutamine expansion mediates pathology by modulating the native protein interactions of the disease protein, we sought to characterize the endogenous ATXN1 protein complexes in mouse cerebellum and identify ATXN1-associated proteins by biochemical copurification from stable cell lines. We report that ATXN1 isolated from mouse cerebellum predominantly associates into large complexes containing the mammalian homolog of *Drosophila* Capicua (CIC), a transcriptional repressor containing a Sox-like high mobility group (HMG) box. Both major isoforms of CIC (CIC-L and CIC-S) are subunits of these complexes. We demonstrate that expression of polyglutamine-expanded ATXN1 alters the repressor activity of CIC, establishing a functional link between the two proteins. Finally, we provide evidence that SCA1 neuropathology depends on incorporation of polyglutamine-expanded ATXN1 into its native CIC-containing complexes.

RESULTS

ATXN1 and CIC Associate into Large Protein Complexes

To identify the major ATXN1 protein complexes in vivo, we examined soluble ATXN1-associated complexes in wild-type mouse cerebellum using gel-filtration and ion exchange chromatography. Gel filtration revealed that the majority of endogenous wild-type ATXN1 (~75%) elutes as large protein complexes (estimated size ~1.8 MDa) (Figures 1A and 1B). Only about 25% of ATXN1 elutes as smaller protein complexes (observed as a shoulder on the larger complexes elution profile, estimated size ~300 kDa) (Figure 1B, right panel).

To identify proteins that interact with ATXN1 in its native complexes, we purified ATXN1-associated proteins by tandem affinity purification (TAP) (Rigaut et al., 1999) and mass spectrometry (Figure S1). We found two novel interacting proteins with apparent molecular masses of ~160 kDa and ~250 kDa, both corresponding to the human homolog of *Drosophila* Capicua (Cic). Northern blot analysis of mouse brain RNA for *Cic* identified two major transcripts (Figure S5A) corresponding to two *Cic* mRNA transcripts predicted to encode proteins of 258 kDa for CIC-L and 164 kDa for CIC-S (Figure S2A). We also identified these alternatively spliced *CIC* mRNA transcripts for both human and *Drosophila* (Figures S2A and S2B). To detect the endogenous CIC protein, we generated antisera against the common C-terminal region of the mouse CIC isoforms (Figure S3A). This antibody specifically recognized CIC-L and CIC-S from mouse cerebellar and HeLa cell extracts (Figures 1 and S3B).

To determine whether CIC is a stable ATXN1-interacting partner, we analyzed the elution profile of CIC by gel-filtration chromatography. We observed that CIC-S and CIC-L coeluted with the large ATXN1 protein complexes (Figures 1A and 1B). Quantification of the relative elution profiles of CIC and ATXN1 using 1 ml fractions, which allows the entire profile to be analyzed on a single gel, revealed a near perfect match between the elution profiles of CIC and the large ATXN1 complexes (Figure 1B).

If CIC and ATXN1 are components of the same protein complexes, loss of ATXN1 will alter the elution profiles of CIC. Indeed, we found that elution of the CIC isoforms is shifted toward later fractions in cerebellar extracts from *Sca1* null mice (Figure S4). Furthermore, we observed a strict cofractionation of ATXN1 with the CIC isoforms using anion exchange chromatography (Figure 1C). Although no significant population of ATXN1 fractionated independently of CIC, we did detect low levels of ATXN1 in the flow-through fractions in the absence of detectable CIC (data not shown), suggesting the smaller ATXN1 complexes have minimal binding to the column matrix.

In sum, the nearly identical elution patterns of the large ATXN1 complexes with CIC-L and CIC-S, and the shift of the CIC profiles in the absence of ATXN1, suggest that the majority of endogenous CIC in the mouse cerebellum stably associates into ATXN1-CIC protein complexes. Also, the smaller ATXN1 protein complexes likely do not contain CIC.

ATXN1 and CIC Interact In Vivo and Colocalize in the Adult Mouse Brain

To determine whether ATXN1 and CIC interact in the tissue most vulnerable in SCA1, we performed coimmunoprecipitation (coIP) of cerebellar extracts from wild-type

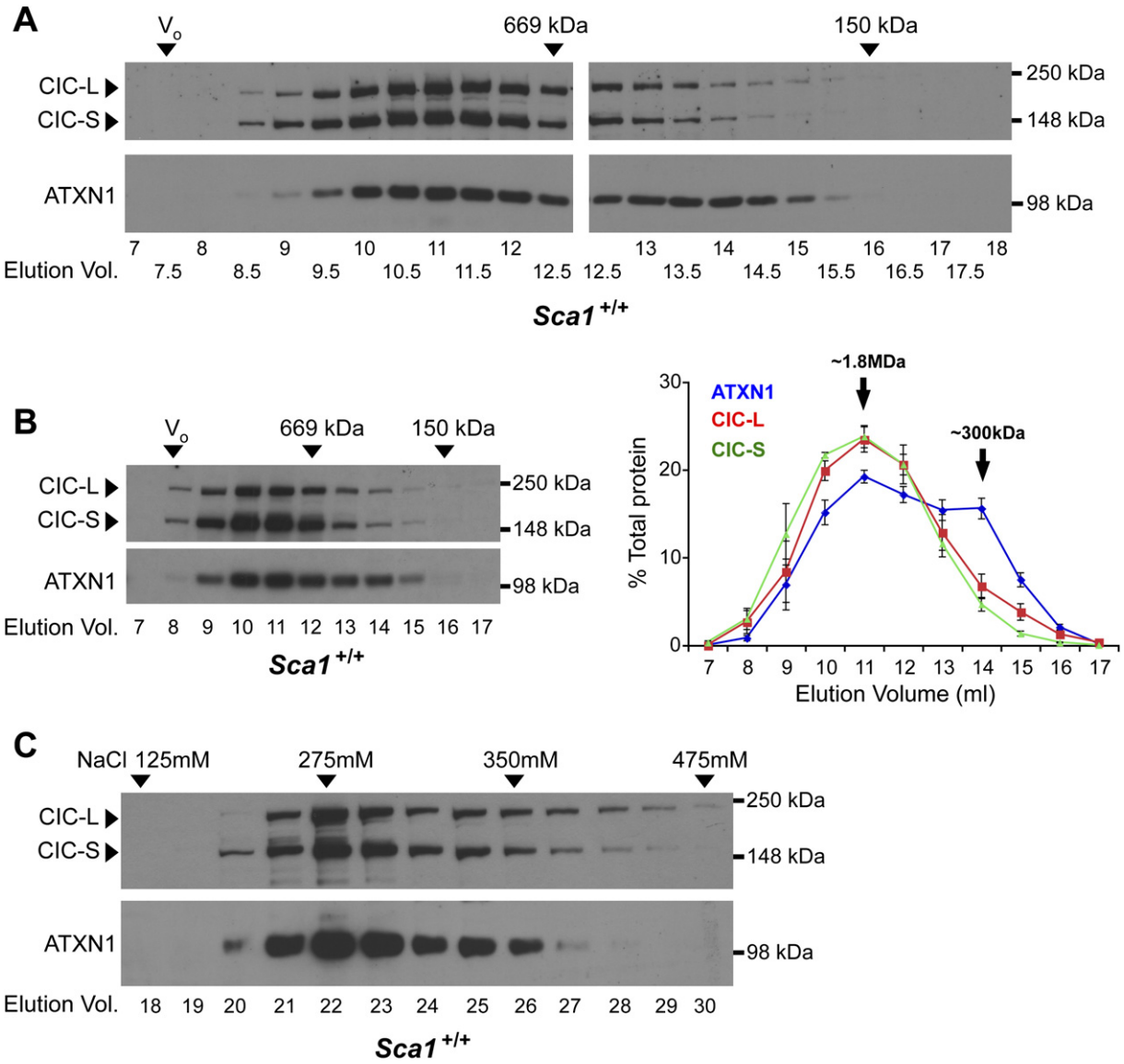

Figure 1. ATXN1 Forms Complexes with CIC in Wild-Type Mouse Cerebellum

(A) Representative westerns of 0.5ml gel-filtration fractions of wild-type mouse cerebellar extracts analyzed for ATXN1 and CIC isoforms (CIC-L and CIC-S).

(B) Representative westerns of 1.0 ml gel-filtration fractions of wild-type cerebellar extracts analyzed for CIC and ATXN1. Right panel illustrates the elution profiles for each protein plotted as the average percent protein (± standard error) in each fraction from four independent extracts. The total signal in each fraction (measured by densitometry) is divided by the total signal of that protein in all the fractions to determine the percentages shown in the panel. The column void volume (V_o), gel-filtration standards thyroglobulin (669 kDa) and ADH (150 kDa), and elution volume (ml) of each collected fraction are indicated.

(C) Representative westerns of monoQ fractions from wild-type cerebellar extracts analyzed for CIC and ATXN1; the approximate eluting NaCl concentration of selected fractions and elution volume (ml) of each collected fraction are indicated.

and *Sca1* null mice using anti-ATXN1 antibody (11NQ). The anti-ATXN1 antibody specifically immunoprecipitated both CIC isoforms from cerebellar extracts of wild-type but not *Sca1* null mice, indicating that CIC and ATXN1 interact in vivo (Figure 2A; input and loading controls for this coIP are in Figure 3A). This is in agreement with our recent work, in which we identified CIC as a binding partner of ATXN1 in an unbiased yeast two-hybrid screen (Lim et al., 2006).

Having established the ATXN1-CIC interaction, we compared their expression patterns in mouse brain. Northern blot analysis showed that the *Cic* isoforms are highly

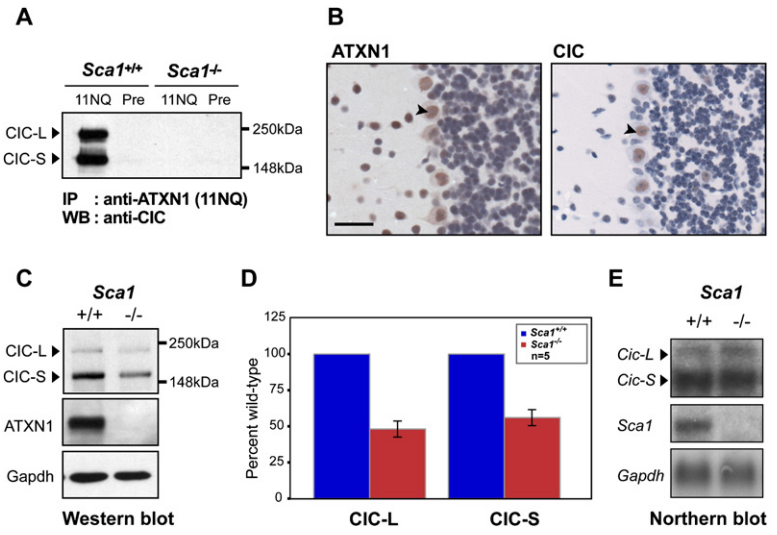

Figure 2. Coexpression and CoIP of CIC and ATXN1 and Reduction of CIC Protein Levels in the Absence of ATXN1

(A) Mouse ATXN1 and the two CIC isoforms coIP from cerebellar extracts of wild-type (*Sca1*$^{+/+}$) but not *Sca1* null (*Sca1*$^{-/-}$) mice. The coIP was performed with anti-ATXN1 antibody (11NQ) and immunoblotted with anti-CIC antibody. Preimmune serum served as the negative control (input and loading controls are in Figure 3A).

(B) Immunohistochemistry of adult mouse brain for ATXN1 (left panel) and CIC (right panel). Both ATXN1 and CIC are abundant in nuclei of Purkinje cells (arrowhead). Scale bar = 33.6 μm.

(C) SDS-PAGE of cerebellar extracts from *Sca1*$^{+/+}$ and *Sca1*$^{-/-}$ mice, analyzed by western blot for CIC-L, CIC-S, wild-type ATXN1 (ATXN1[2Q]), and the control Gapdh.

(D) Graphs show the normalized levels of CIC-L and CIC-S in cerebellar extracts from *Sca1*$^{-/-}$ versus *Sca1*$^{+/+}$ mice; mean relative levels (wt = 100%) and standard error are shown ($n = 5$, t test $p < 0.001$).

(E) Northern analysis of total RNA extracted from *Sca1*$^{+/+}$ and *Sca1*$^{-/-}$ cerebella, probed for *Cic*, *Sca1*, and *Gapdh*.

expressed in the cerebellum and olfactory bulb (Figure S5A, upper panel). In situ hybridization of adult mouse brain for *Cic* and *Sca1* revealed strikingly similar expression patterns, with high expression in Purkinje cells and in the hippocampus (Figures S5B–S5I). Immunohistochemistry for CIC and ATXN1 also displayed matching protein expression patterns in most brain regions (data not shown). Importantly, both proteins are highly expressed in the nuclei of the Purkinje cells, where polyglutamine-expanded ATXN1 does the most damage (Figure 2B).

To look for interdependence between CIC and ATXN1, we examined CIC protein levels in *Sca1* null mice. We found that both CIC isoforms had significantly reduced levels in *Sca1* null mouse cerebellum (Figures 2C and 2D) and cerebrum (data not shown). As the mRNA levels of the *Cic* isoforms are unaltered in *Sca1* null mice, the dependency of CIC on ATXN1 is posttranscriptional (Figure 2E). Thus, CIC is less stable in the absence of ATXN1 in vivo.

The Majority of CIC Associates with ATXN1 In Vivo

To assess the degree of CIC association with ATXN1 in vivo, we immunoprecipitated ATXN1 from cerebellar extracts and measured the codepletion of CIC from the post-IP supernatants. Both CIC isoforms were substantially depleted following ATXN1 immunodepletion, demonstrating that the majority of endogenous CIC associates with ATXN1 (Figure 3A). In contrast, the levels of neither Gapdh (data not shown) or AKT (Figure 3A), an ATXN1 kinase thought to interact transiently with ATXN1 (Chen et al., 2003), are decreased by ATXN1 immunodepletion. Averaging data from independent experiments, we observed that when an average of 72% of ATXN1 is immunodepleted, an average of 62% of CIC-L and 56% of CIC-S are codepleted from the cerebellar extracts. We therefore estimate that ~80% of endogenous CIC associates with ATXN1 (Figure 3B). The depleted CIC isoforms are found in the pellet of the immunoprecipitate (see for example Figure 2A).

A Conserved Domain of CIC Interacts with the AXH Domain of ATXN1

To establish whether CIC also interacts with mutant forms of ATXN1, we performed immunoprecipitation on lysates from HeLa cells transiently transfected with variants of FLAG-tagged ATXN1 containing 2Q, 82Q, or 82Q with a S776A mutation (which abolishes the interaction of ATXN1 with 14-3-3) or 2Q with a deletion of the AXH domain. We found that both endogenous CIC isoforms coimmunoprecipitated with each of these ATXN1 variants, except the one lacking the AXH domain (Figure 3C). We conclude that the ATXN1-CIC interaction requires the AXH domain and is independent of 14-3-3 binding.

To identify the domains responsible for interaction between the two proteins, we performed yeast two-hybrid interaction assays using a series of ATXN1 and CIC deletion constructs. We found that two N-terminal fragments of CIC-S (amino acids 1–300 and 1–205) interact with the C-terminal half of ATXN1 and that the AXH domain of ATXN1 is sufficient for its interaction with CIC (Figure 3D). To further map the ATXN1 binding domain of CIC, we generated serial deletions at the N terminus of mouse CIC-S for pull-down assays with GST-tagged full-length wild-type ATXN1 (Figures S6A and S6B). We

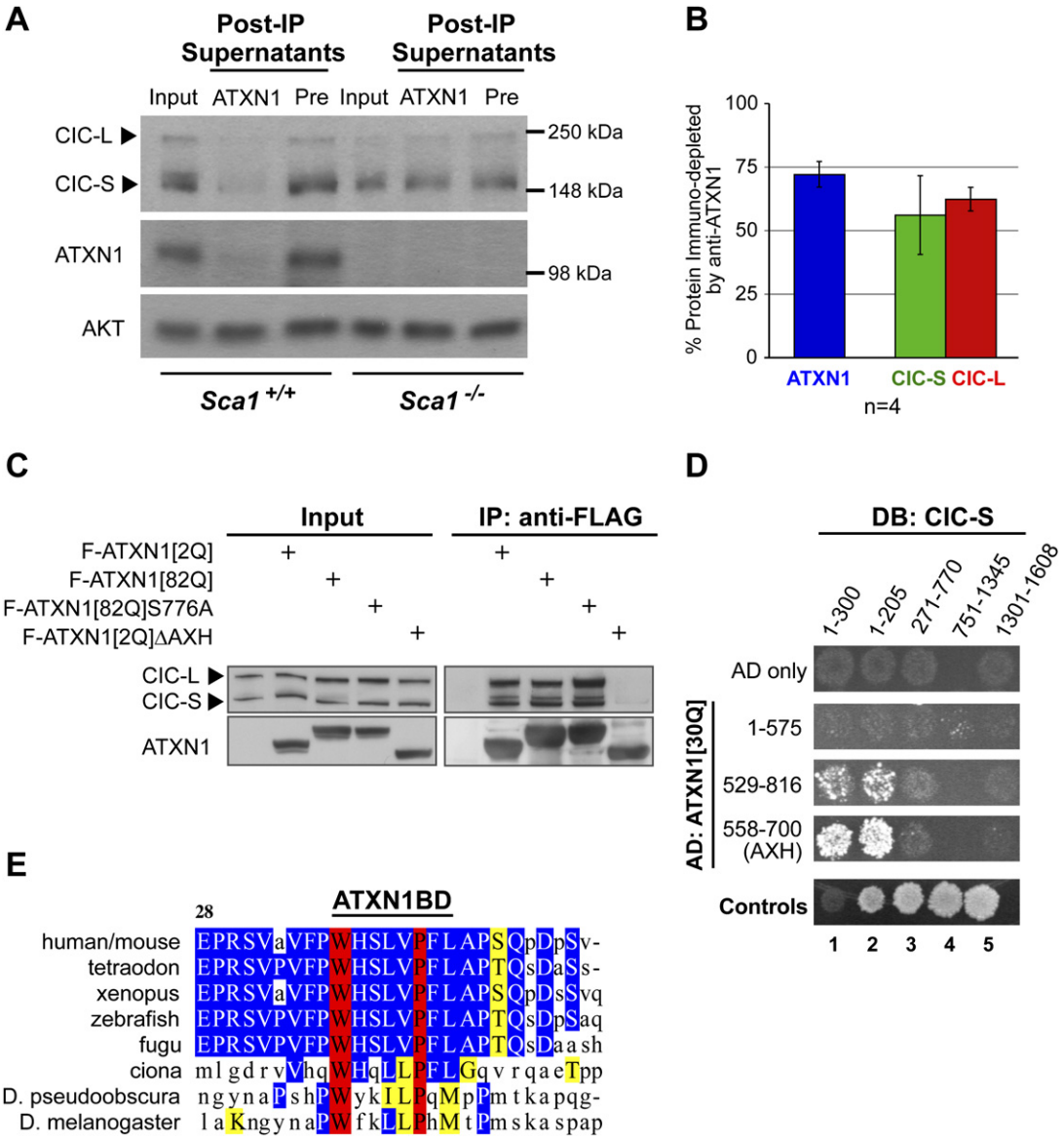

Figure 3. The Majority of CIC Associates with ATXN1 In Vivo

(A) Representative westerns of an immunodepletion experiment of *Sca1*$^{+/+}$ and *Sca1*$^{-/-}$ cerebellar extracts before (input) and after either anti-ATXN1 (ATXN1) or preimmune sera (Pre) IP (Post-IP Supernatants). Blots analyzed for CIC-L, CIC-S, ATXN1, and AKT as indicated at left of each panel.

(B) Average percentage and standard deviation of ATXN1, CIC-L, and CIC-S proteins immunodepleted from four independent cerebellar extracts by anti-ATXN1 IP.

(C) IP of lysates from HeLa cells transfected with variants of FLAG-tagged human ATXN1 containing 2Q (F-ATXN1[2Q]), 82Q (F-ATXN1[82Q]), 82Q with S776A mutation (F-ATXN1[82Q]S776A), or 2Q with the deletion of AXH domain (F-ATXN1[2Q]ΔAXH). The coIP was performed with anti-FLAG conjugated beads and immunoblotted with anti-FLAG for ATXN1 and anti-CIC antibody for the endogenous CIC.

(D) Yeast two-hybrid assays mapping the regions responsible for ATXN1-CIC interaction. AD (activation domain) and DB (DNA binding domain) of Gal4. Controls are the following: lane 1, negative control (DB and AD vectors alone); and lanes 2–5, positive controls.

(E) Sequence alignment of CIC homologs corresponding to amino acids 28–52 of mouse CIC-S reveals a conserved region indicated as ATXN1BD.

narrowed the interaction region to 31 amino acids (amino acids 16–46) of CIC-S (Figure S6C). Comparison of this 31-amino acid sequence across species revealed a conserved stretch of eight amino acids present in both CIC-S and CIC-L isoforms with the consensus sequence WXX(L/I)(V/L)PX(L/M) (Figure 3E). We then confirmed in vitro that human ATXN1 binds to *Drosophila* Cic through the consensus eight amino acids (Figure S6D). ATXN1 and CIC thus appear to be in vivo binding partners that interact directly through evolutionarily conserved domains.

Soluble ATXN1[154Q] and Wild-Type ATXN1 Associate with Similarly Sized Complexes

Having established that polyglutamine-expanded ATXN1 interacts with CIC, we asked whether the expanded polyglutamine tract alters the incorporation of ATXN1 into its native protein complexes. We examined cerebellar extracts from *Sca1*$^{154Q/+}$ animals that express polyglutamine-expanded ATXN1[154Q] from its endogenous locus and are an accurate model of SCA1 (Watase et al., 2002). As previously reported, the levels of soluble expanded protein are significantly lower than wild-type ATXN1 levels in these animals, although expression of the mutant allele is identical to the wild-type allele (Watase et al., 2002). Gel-filtration chromatography of extracts from early symptomatic animals (10–15 weeks of age) revealed that soluble ATXN1[154Q] and wild-type ATXN1 (expressed from the untargeted allele) eluted into the same fractions as ATXN1 from wild-type extracts (Figure 4A). The elution profile of CIC from *Sca1*$^{154Q/+}$ mice is indistinguishable from that seen in wild-type animals (Figure 4A). A subtle change in the elution profile of the smaller ATXN1 complexes (elution fractions from 13 ml to 16 ml) was observed in the mutant animals: both ATXN1[154Q] and wild-type ATXN1 showed a relative loss from elution fractions at 14 ml and beyond, with a corresponding increase in elution fractions at 13 ml and 13.5 ml (estimated size ~500 kDa) compared to wild-type animals (compare Figure 1A to 4A). The basis for this change is unclear at present, but it could represent an alternate conformation of the smaller ATXN1 protein complexes coupled with the slight increase of molecular weight due to polyglutamine expansion. The similar elution patterns of wild-type and expanded ATXN1 by gel-filtration chromatography suggest that polyglutamine expansion does not prevent the incorporation of ATXN1 into its normal endogenous protein complexes.

To confirm that polyglutamine-expanded ATXN1 incorporates into similar complexes as wild-type ATXN1, we analyzed cerebellar extracts from *Sca1*$^{154Q/+}$ animals by anion-exchange chromatography. We found that ATXN1[154Q] coelutes with wild-type ATXN1 and with both CIC isoforms (Figure 4B). The elution profiles of ATXN1, CIC-L, and CIC-S in extracts by anion-exchange chromatography are quite broad; this argues against a single complex of uniform structure and suggests that the ATXN1-CIC protein complexes adopt multiple conformational or compositional states separable by differences in their charge (Figures 1C and 4B).

The S776A Mutation Reduces Incorporation of Mutant ATXN1 into the Large ATXN1-CIC Complexes

We previously showed that mutating serine 776 of ATXN1 to alanine (S776A) dramatically suppresses the neurotoxicity of the polyglutamine-expanded protein in Purkinje cells (Emamian et al., 2003). This mutation causes loss of interaction with the chaperone protein 14-3-3 (Chen et al., 2003). To investigate whether the decrease in pathogenicity correlates with alterations in the ATXN1 complexes in vivo, we compared transgenic mice expressing human polyglutamine-expanded ATXN1[82Q] (Tg-*SCA1[82Q]*) with transgenic mice expressing ATXN1[82Q] with the S776A mutation (Tg-*SCA1*[*82Q*]*S776A*)—both transgenic lines express the ATXN1 variants specifically in cerebellar Purkinje cells at similar levels (Burright et al., 1995; Emamian et al., 2003).

We analyzed cerebellar extracts from Tg-*SCA1*[*82Q*] mice by gel filtration and found that ATXN1[82Q] associates into both large and small protein complexes (Figures 4C and 4E). However, cerebellar extracts from Tg-*SCA1*[*82Q*]*S776A* showed a specific loss of ATXN1[82Q]S776A from the large protein complexes, whereas wild-type ATXN1 had an elution profile similar to wild-type extracts (Figures 4D and 4E). The normal elution pattern of endogenous wild-type ATXN1 suggested that the elution profile of CIC would be similar in Tg-*SCA1*[*82Q*]*S776A* and wild-type animals, and this indeed was the case. Failure of ATXN1[82Q]S776A to incorporate into the large ATXN1-CIC complexes is not due to a general inability of the S776A mutant protein to physically bind CIC, as both endogenous CIC isoforms from HeLa cells can be coimmunoprecipitated with ATXN1, independent of polyglutamine expansion and/or the S776A mutation (Figure 3C). This suggests that the S776 residue of ATXN1 plays a critical role in regulating ATXN1-CIC complex formation in Purkinje cells.

Human Mutant ATXN1 Blocks Cic Function in *Drosophila*

The finding that loss of polyglutamine-expanded ATXN1 from its large native complexes correlates with a lack of neuronal dysfunction in Tg-*SCA1*[*82Q*]*S776A* suggests that mutant ATXN1 might cause toxicity by altering the function of its native complexes. We hypothesized that polyglutamine-expanded ATXN1 affects the function of its native complex by interfering with the function of CIC. To explore this possibility we turned to *Drosophila*, where the function of Cic has been investigated in vivo.

We performed genetic interaction studies to determine whether Cic can modify ATXN1 phenotypes and whether ATXN1 interferes with the repressor function of Cic in vivo. We previously showed that expression of human *SCA1*[*82Q*] in the *Drosophila* eye causes a degenerative phenotype (Fernandez-Funez et al., 2000). To test whether *Drosophila cic* modifies the *SCA1*[*82Q*] eye phenotype, we generated transgenic flies expressing *Drosophila cic*. As expected, flies coexpressing *SCA1*[*82Q*] and a control gene (*GFP*) at 29°C show ommatidial disorganization and fusion as well as interommatidial bristle loss (Figures 5A and 5B). Although overexpression of *cic* also causes mild ommatidial disorganization (Figure 5D), coexpression of *cic* and *SCA1*[*82Q*] ameliorates the ommatidial disorganization of the fly eye and partially restores bristles (Figure 5C), demonstrating that Cic modulates ATXN1's toxicity.

To examine *SCA1*[*82Q*] eye phenotypes in the context of *cic* mutations, we crossed *SCA1*[*82Q*] flies with *cic*^{2}

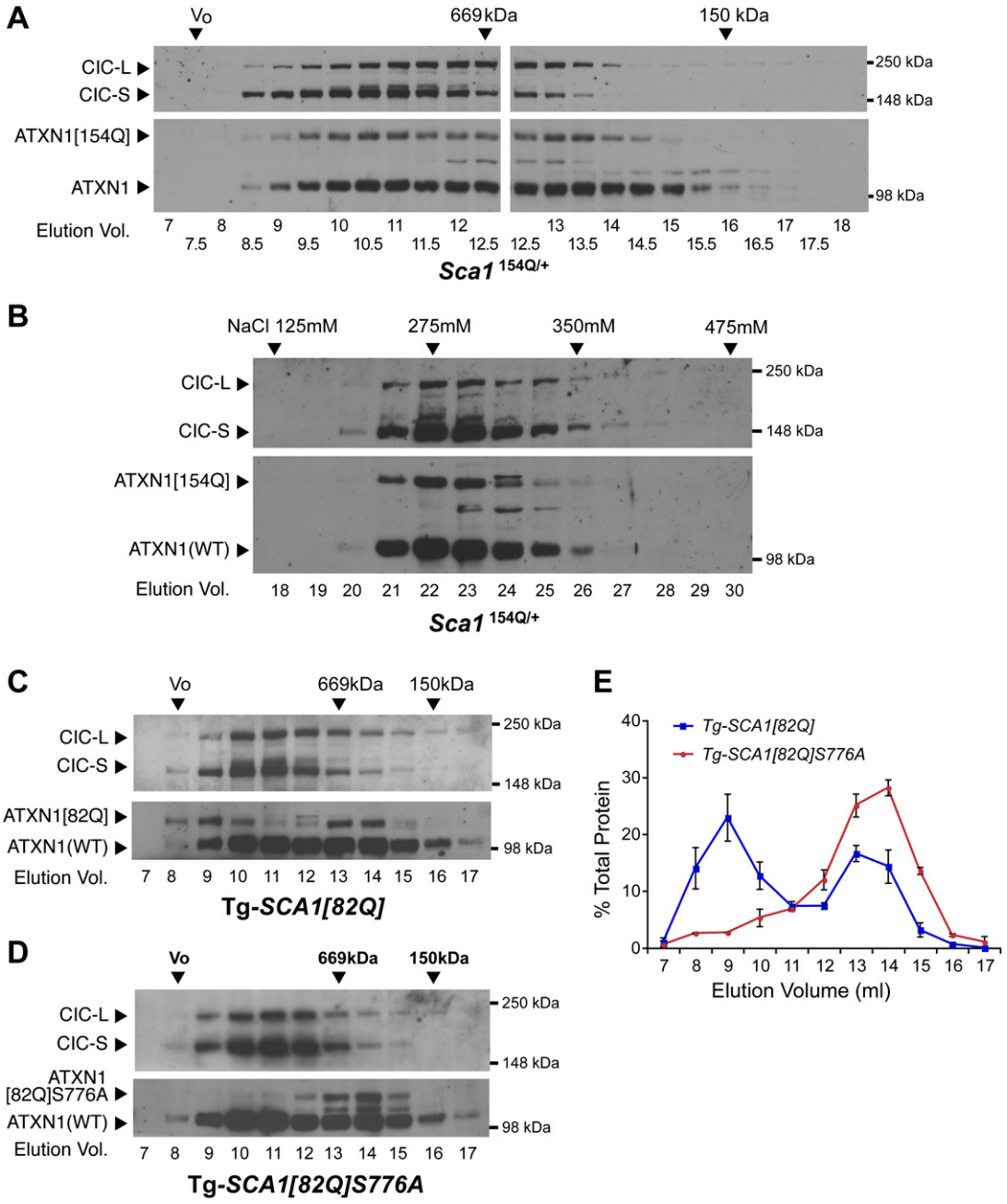

Figure 4. Polyglutamine-Expanded ATXN1 Associates with CIC in Its Native Complexes unless It Carries the S776A Mutation that Suppresses Its Toxicity

(A) Representative westerns of 0.5 ml gel-filtration fractions of *Sca1*$^{154Q/+}$ mouse cerebellar extracts analyzed for CIC, ATXN1[154Q], and wild-type ATXN1.

(B) Representative westerns of monoQ fractions from *Sca1*$^{154Q/+}$ cerebellar extracts analyzed for CIC, ATXN1[154Q], and wild-type ATXN1.

(C and D) Representative westerns of gel-filtration fractions from Tg-*SCA1*[*82Q*] (C) or Tg-*SCA1*[*82Q*]*S776A* (D) cerebellar extracts, analyzed for CIC, wild-type ATXN1, ATXN1[82Q], or ATXN1[82Q]S776A protein. The large complexes formed by transgenic human ATXN1[82Q] proteins are shifted toward earlier fractions compared to the mouse ATXN1 complexes, likely due to intrinsic differences between the mouse and human proteins. The key finding is that the large complexes formed by ATXN1[82Q] are almost absent for ATXN1[82Q]S776A.

(E) Fractionation profiles comparing the mutant ATXN1 proteins analyzed as in (C and D), plotted as the average percent of mutant ATXN1 proteins (± standard error) in each fraction averaged from two independent extracts of each genotype. The total signal in each fraction (measured by densitometry of the protein band) is divided by the total signal for that protein in all the fractions to determine the percentages shown in the panel.

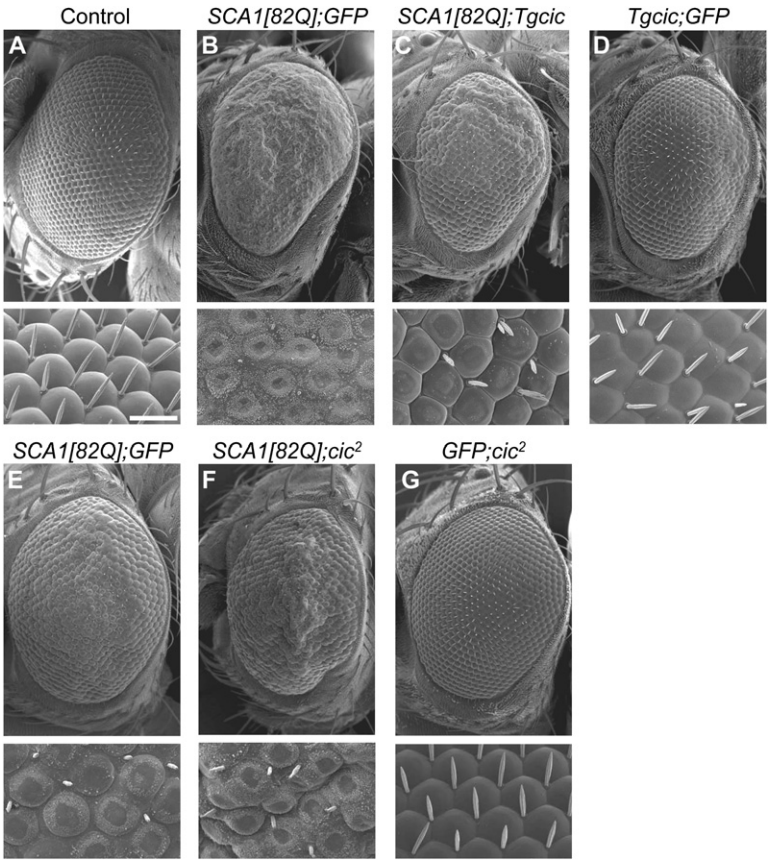

Figure 5. *Drosophila* Cic Modifies Human ATXN1[82Q]-Induced Eye Phenotypes

Overexpression of *Drosophila* Cic suppresses ATXN1-induced eye abnormalities.

(A)–(D) Eye scanning electron microscopy (SEM) of (A) yw; gmr-*GAL4/UAS-GFP* (control), (B) *UAS-SCA1*[*82Q*]*F7/yw*; *gmr-GAL4/UAS-GFP*, (C) *UAS-SCA1*[*82Q*]*F7/yw*; *gmr-GAL4/+;UAS-cic/+*, and (D) *gmr-GAL4/UAS-GFP;UAS-cic/+*. ATXN1-induced eye phenotypes are enhanced in cic^2/+ background.

(E)–(G) Eye SEM of (E) *UAS-SCA1*[*82Q*]*F7/yw*; *gmr-GAL4/UAS-GFP,* (F) *UAS-SCA1*[*82Q*]*F7/yw*; *gmr-GAL4/+;* cic^2/+, and (G) *gmr-GAL4/UAS-GFP*; cic^2/+. Flies from (A)–(D) were raised at 29°C and (E)–(G) at 25°C. Scale bar = 10 μm.

mutant flies, an EMS-induced null allele (Roch et al., 2002). At room temperature, *SCA1*[*82Q*] flies show milder ommatidial disorganization due to decreased expression of the disease protein (Figure 5E). But loss of one functional allele of *cic*, which by itself causes no eye phenotype, worsened ommatidial disorganization in these *SCA1*[*82Q*] flies (compare Figure 5E to 5F).

In *Drosophila*, Cic functions as a transcriptional regulator important for various developmental processes (Atkey et al., 2006; Jimenez et al., 2000; Roch et al., 2002). In the developing wing, Cic represses several wing-vein specific genes, *argos* (*aos*), *ventral veinless* (*vvl*), and *decapentaplegic* (*dpp*), and *cic* mutants develop ectopic and thickened wing veins (Roch et al., 2002). This provided an excellent opportunity to study the effects of ATXN1 on Cic's endogenous repressor function, because expression of human *SCA1*[*82Q*] and *Drosophila Atxn1* in the wing also causes wing-vein phenotypes (Tsuda et al., 2005).

Using a wing-pouch specific driver (C5-GAL4) to express *SCA1*[*82Q*], we observed smaller wings with a thicker L3 vein, a missing posterior crossvein, and ectopic vein formation (Figure 6A). These phenotypes were more prominent at the posterior part of the wing, where the expression of the transgene was highest (Figure 6N). The higher expression of *SCA1*[*82Q*] in males (due to insertion of the transgene on the X chromosome) produced atrophic wings (Figure 6E). Animals heterozygous for the cic^2 null allele (cic^2/+) did not show a wing phenotype (Figure 6C), but C5-GAL4-driven expression of *SCA1*[*82Q*] in the cic^2/+ background showed more prominent L3 vein thickening and increased ectopic vein formation in the posterior part of the interveins than overexpression of *SCA1*[*82Q*] alone (Figures 6A and 6B).

Because mutant ATXN1-induced wing-vein abnormalities were augmented in the cic^2/+ background, we tested whether increasing Cic levels could suppress these phenotypes. Although *cic* overexpression caused the loss of veins at the posterior part of the wing (Figures 6G and 6K), as predicted from its role in wing-vein development, it restored overall wing integrity in flies expressing *SCA1*[*82Q*] (compare Figure 6E to 6F and Figure 6I to 6J). Importantly, flies overexpressing *SCA1*[*82Q*]*ΔAXH* did not develop these wing abnormalities (Figure 6H). This demonstrates that *SCA1*[*82Q*] wing-vein phenotypes are dependent on the AXH domain, supporting our finding that this domain mediates ATXN1-CIC interactions. Therefore, the mutant ATXN1-induced wing-vein abnormalities are likely acting via the *cic* pathway.

To confirm that *SCA1*[*82Q*] modifies *cic* pathway function, we examined the expression of a *cic* downstream target gene, *aos,* using an *aos*-promoter *LacZ* reporter line (aos^{W11}). In the wild-type pupal wing at 36 hr after puparium formation (APF), the expression of *aos* was confined

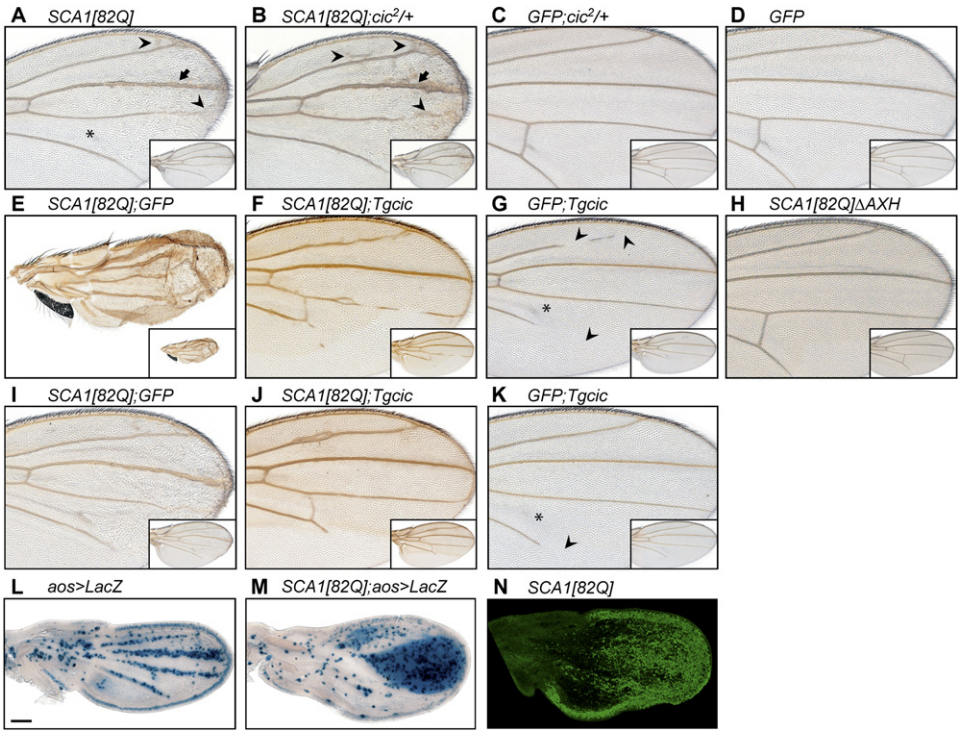

Figure 6. Genetic Interaction of *Drosophila cic* and Human *ATXN1[82Q]* in *Drosophila* Wing

Wing abnormality phenotypes of *SCA1*[*82Q*] transgenic flies are modified by hypomorphic and transgenic alleles of *cic*; representative wings are shown for each genotype.

(A)–(D) A strong hypomorphic allele of *cic* (*cic*^{2}) enhances human ATXN1-induced wing-vein abnormalities under the control of C5-GAL4 driver. In (A) is the following: *UAS-SCA1*[*82Q*]/+; *C5-GAL4*/+ flies show thickening of L3 vein (arrow), extra veins formation (arrowhead), and a missing posterior crossvein (*). In (B) is the following: *UAS-SCA1*[*82Q*]/+; *C5-GAL4*/*cic*^{2} transgenic flies display further thickening of the L3 vein (arrow) and increased extra vein formation (arrowhead). Controls *UAS-GFP*/+; *C5-GAL4*/*cic*^{2} (C) and *UAS-GFP*/+; *C5-GAL4*/+ (D) show a normal wing phenotype.

(E)–(K) The *UAS-cic* flies (Tg*cic*) suppress ATXN1-induced wing abnormalities. In (E) is the following: male wing of *UAS-SCA1*[*82Q*]/Y; *UAS-GFP*/+; *C5-GAL4*/+ and (I) female wing of *UAS-SCA1*[*82Q*]/+; *UAS-GFP*/+; *C5-GAL4*/+ show dosage dependent phenotypes of the wing abnormalities and both are suppressed by overexpression of *cic* (F and J). Both male (G) and female (K) *UAS-GFP*/*UAS-cic*; *C5-GAL4*/+ show missing veins (arrowheads) and crossvein (*) phenotype. (H) AXH deletion in *UAS-SCA1*[*82Q*]*ΔAXH*/+; *C5-GAL4*/+ flies abolishes the wing abnormality induced by the polyglutamine expansion.

(L)–(M) ATXN1[82Q] derepresses *aos* expression. LacZ staining of 36 hr APF wings of *aos*^{w11}/*C5-GAL4* (L) and *UAS-SCA1*[*82Q*]/+; *aos*^{w11}/*C5-GAL4* (M).

(N) Immunofluorescence staining for ATXN1 of *UAS-SCA1*[*82Q*]/+; *aos*^{w11}/*C5-GAL4* wing at 36 hr after puparium formation. Scale bar = 268 μm.

to the vein region as shown by LacZ staining (Figure 6L). In contrast, *aos* expression was derepressed in flies expressing *SCA1*[*82Q*] in the wing pouch under the control of the C5-GAL4 driver (Figure 6M). Furthermore, expansion of the *aos* expression domain correlated with the expression of *SCA1*[*82Q*] (Figure 6N). These data indicate that overexpression of ATXN1[82Q] impairs Cic function, probably through direct protein-protein interactions, relieving *aos* repression by Cic.

Differential Effects of Wild-Type and Mutant ATXN1 on CIC Transcriptional Repression

Having established that mutant ATXN1 interferes with the function of Cic as a repressor in *Drosophila*, we asked whether ATXN1 affects the function of CIC in a mammalian system. We performed luciferase assays using a reporter construct bearing six copies of the recently identified CIC binding site (CBS) (Kawamura-Saito et al., 2006). We observed a moderate decrease in luciferase activity when HEK293T cells were transfected with a small amount (2.5 ng) of CIC-S, whereas coexpression with ATXN1[2Q] decreased luciferase activity 2-fold (Figure 7). The synergistic effect of ATXN1 and CIC-S coexpression on the transcriptional repression activity of CIC-S required the AXH domain. Interestingly, the ability of ATXN1[82Q] to repress transcription was impaired in comparison with ATXN1[2Q] only when CIC-S was cotransfected (Figure 7). These data demonstrate a direct link between the transcriptional repression activities of CIC and ATXN1 and show that polyglutamine expansion alters functions that depend on the interaction of these proteins.

DISCUSSION

The data presented in this study demonstrate that the majority of cerebellar ATXN1 associates into a group of large

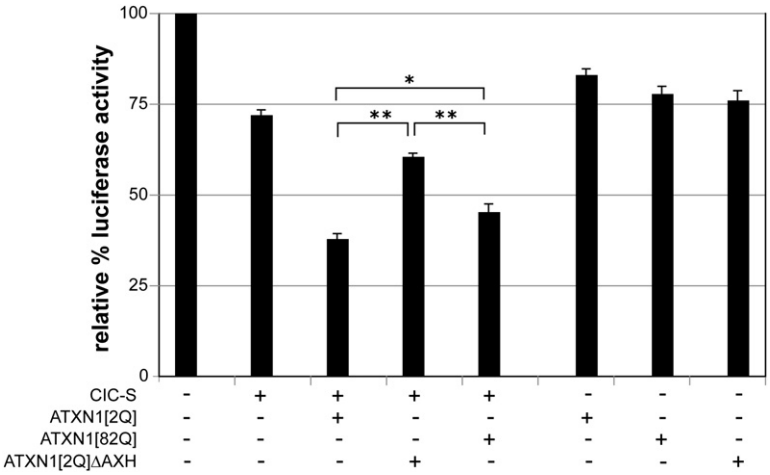

Figure 7. Synergistic Repression of Luciferase Activity by ATXN1 and CIC

HEK293T cells transfected with a luciferase reporter that has CIC binding sites and expression plasmids (CIC-S and ATXN1 variants) in duplicate. The luciferase data are expressed as mean percentage of luciferase activity (± standard error) relative to the reporter alone ($n \geq 4$, t test * $p < 0.05$ and ** $p < 0.005$).

complexes that contain the transcriptional repressor CIC. We found that a nonpathogenic form of polyglutamine-expanded ATXN1, the S776A mutant, does not associate with the large ATXN1-CIC complexes, indicating that incorporation of polyglutamine-expanded ATXN1 into these complexes is important for its toxicity. Our findings that the majority of endogenous CIC associates with ATXN1 and that CIC levels are decreased in the absence of ATXN1 underscore the functional relationship between these two proteins. Lastly, we demonstrate that polyglutamine-expanded ATXN1 alters the repressor activity of CIC in vitro and in vivo. We conclude that ATXN1 acts in a transcriptional repressor complex and that polyglutamine-expanded ATXN1 exerts neurotoxicity through its native complexes containing CIC rather than through aberrant interactions with novel proteins. The complementary approaches we have taken permitted us to go beyond the identification of binary protein-protein interactions and to elucidate pathologically relevant alterations in native protein complexes harboring the disease protein.

Previous work from our lab and others has identified several ATXN1-interacting proteins and genetic modifiers of SCA1 phenotypes that are involved in transcriptional regulation, including silencing mediator of retinoid and thyroid hormone receptors (SMRT), polyglutamine binding protein 1 (PQBP1), and growth factor independent-1 (Gfi-1) (Fernandez-Funez et al., 2000; Okazawa et al., 2002; Tsai et al., 2004; Tsuda et al., 2005). It remains unknown, however, whether these proteins form stable complexes or transiently interact with ATXN1. For example, the interaction of ATXN1 with the Senseless/Gfi-1 proteins leads to their destabilization and is expected to be transient (Tsuda et al., 2005). Consistent with this, we did not find mouse Gfi-1 or SMRT associated with the major ATXN1 complexes in vivo (data not shown).

CIC contains a Sox-like high mobility group (HMG) box and likely acts as a transcriptional repressor (Atkey et al., 2006; Jimenez et al., 2000; Roch et al., 2002). Given that ATXN1 lacks sequence-specific DNA binding activity (de Chiara et al., 2005), CIC could be involved in directing ATXN1 to gene targets for repression. Our studies clearly show that ATXN1 has a synergistic effect on the transcriptional repressor activity of CIC that is partially compromised by the polyglutamine expansion. One possible explanation is that polyglutamine expansion alters the conformational state of the ATXN1 protein, which in turn alters the conformational or functional state of the ATXN1-CIC complex. Identifying transcriptional targets of the ATXN1-CIC complexes, particularly in the selectively vulnerable Purkinje cells, will likely reveal specific pathways that are critical for disease pathogenesis.

Our findings for SCA1 may apply to other polyglutamine diseases. Indeed, altered interactions of mutant Huntingtin with HAP1 and $p150^{Glued}$ have been associated with impaired axonal trafficking of BDNF (Gauthier et al., 2004). Thus, changes in native complexes could be one of the final steps of commonality in polyglutamine disease pathogenesis. Beyond this step, we suggest that the features particular to each disease are determined by both transient and stable protein interactions and the susceptibility of such interactions to conformational or functional alterations by the soluble polyglutamine-expanded disease protein. Determining how polyglutamine expansion alters the activity of the disease protein could enable therapeutic approaches to counter neuropathology by either blocking specific interactions that mediate selective neurotoxicity or modulating the downstream events of such interactions. Beyond polyglutamine diseases, it is becoming clear that elevated levels of even wild-type amyloid precursor protein and wild-type α-synuclein cause dementia and Parkison disease, respectively, just as overexpression of wild-type ATXN1 produces neurodegeneration (Eriksen et al., 2005; Fernandez-Funez et al., 2000; Rovelet-Lecrux et al., 2006). Identifying these native protein complexes could point to key effectors or modifiers of the disease phenotypes.

EXPERIMENTAL PROCEDURES

Column Fractionation and Analysis

Chromatography was carried out at 4°C using the Amersham Pharmacia LCC-500 FPLC system. Unless stated otherwise, the data shown represent >10 independent runs for each genotype analyzed. Cerebellar extracts were prepared fresh by dounce homogenization of one to two cerebella from age-matched mice (≤16 weeks) dissected in TST buffer (50mM Tris, pH 8, 75mM NaCl, 0.5% Triton X-100, 1mM PMSF, and protease inhibitors). Seven hundred microliters were loaded for FPLC. Gel filtration was a Superose 6 10/300 GL column (Amersham Pharmacia) equilibrated in buffer (50 mM Tris, pH 8, 20mM NaCl) at 0.4 ml/min. Fractions were collected every 0.5 ml or 1 ml volume, column void volume was 7.7ml, and elution volumes of gel-filtration standards were 12.4 ml for thyroglobulin (669 kDa), 15.8 ml for ADH (150 kDa), and 19.2ml for cytochrome C (12.4 kDa). Anion exchange was a MonoQ 5/5 HR column (Amersham Pharmacia) equilibrated in buffer (50 mM Tris, pH 8, 50 mM NaCl); after washing the column with ~13 column volumes of the same buffer, bound proteins were eluted by a 20 ml linear NaCl salt gradient from 50 mM to 600 mM NaCl in 50 mM Tris, pH 8 at 1ml/min; 1 ml fractions were collected. All fractions were supplemented with protease inhibitors and immediately prepared for SDS-PAGE.

Immunoprecipitation

Protein (0.5 mg) from cerebellar extracts in 200 μl TST buffer were diluted with 800 μl of cold PBS (Input). Two microliters of Anti-ATXN1 (11NQ) serum or preimmune serum was added and incubated overnight at 4°C. IP was performed with BSA-blocked protein G sepharose beads, and the immunodepleted supernatant (Post-IP Supernatant) was saved, and the pellet (IP pellet) was resuspended in sample buffer following three to six washes with cold PBS. Input, post-IP supernatant, and IP pellets were analyzed by SDS-PAGE and western blot.

RNA and Protein Analyses

RNA isolation and northern blot was as described (Emamian et al., 2003). The *Gapdh* probe is a 486 bp PCR fragment of the mouse cDNA; the *Cic* probe is a 530 bp SpeI fragment of the coding region common to both isoforms, and the *Sca1* probe is as clone corresponding to mouse cDNA.

Guinea pig polyclonal anti-CIC serum was generated by immunizing with bacterially expressed HIS-tagged C-terminal 214 amino acids of CIC (Cocalico). Mouse monoclonal anti-FLAG M2 (Sigma), rabbit polyclonal anti-ATXN1 (11750VII and 11NQ), mouse monoclonal anti-GAPDH (Advance Immunochemical), and rabbit polyclonal anti-AKT (Cell Signaling) were used. SDS-PAGE western blotting and immunohistochemistry followed standard protocols (Chen et al., 2003; Watase et al., 2002). Yeast two-hybrid assay was performed as previously described (Lim et al., 2006).

Fly Strains

Drosophila cic cDNA was inserted in the pUAST vector to generate *UAS-cic* transgenic lines. Other strains used were *UAS-SCA1[82Q]* (F7, N35Y, M6) (Fernandez-Funez et al., 2000), *UAS-SCA11[82Q]ΔAXH* (Tsuda et al., 2005), *C5-GAL4* (Yeh et al., 1995), *UAS-GFP* (H. Bellen), cic^{2} (Roch et al., 2002), aos^{W11}, and *yw* (Bloomington stock center).

X-Gal Staining and SEM

Thirty-six hour APF pupae were fixed in 0.3% glutaraldehyde solution for 10 min. The pupal wings were dissected in 1XPBS and washed in 1XPBS for 15–30 min before staining in 0.3% X-gal in Fe/NaP solution for 3 hr at 37°C. Processing of *Drosophila* for SEM was performed as previously described (Fernandez-Funez et al., 2000). Image acquisition was taken from MD Anderson SEM core.

Luciferase Assay

Cotransfected were 1.8 × 10^{5} HEK293T cells in 24-well plates using Lipofectamine 2000 (Invitrogen) with 50 ng of the pGL3-Promoter (Promega) containing six copies of CIC binding sites (TGAATGAA or TGAATGGA) (Kawamura-Saito et al., 2006), 10 ng of pRL-TK, and 2.5 ng of expression plasmids as indicated. The total amount of DNA transfected was kept constant by adding pcDNA3.1(−) (Invitrogen). Luciferase activities were measured using the dual luciferase reporter assay system (Promega).

Supplemental Data

Supplemental Data include six figures and Supplemental References and can be found with this article online at http://www.cell.com/cgi/content/full/127/7/1335/DC1/.

ACKNOWLEDGMENTS

We are grateful to Yuchun He for generating the Cic transgenic fruit flies, to Christina Thaller for in situ hybridization, to Bobby Antalffy for immunohistochemistry, to Sukeshi Vaishnav for mouse genotyping, to Jordi Casanova for providing *Drosophila cic* flies and cDNA constructs, and to Dong Zhang for providing reagents and advice for TAP. Special thanks to Hugo Bellen, Hamed Jafar-Nejad, Patrik Verstreken, Adriano Flora, Jennifer Gatchel, Paolo Moretti, and Juan Crespo-Barreto for many insightful discussions and Vicky Brandt for editorial input. This work was supported by NINDS NS27699 (to H.Y.Z.), NS22920 and NS45667 (to H.T.O.), and NICHD HD024064 (to the BCM-MRRC). A.B.B. was a Postdoctoral Fellow of the Hereditary Disease Foundation. H.Y.Z. is an HHMI investigator.

Received: February 21, 2006
Revised: August 15, 2006
Accepted: November 21, 2006
Published: December 28, 2006

REFERENCES

Atkey, M.R., Lachance, J.F., Walczak, M., Rebello, T., and Nilson, L.A. (2006). Capicua regulates follicle cell fate in the Drosophila ovary through repression of mirror. Development *133*, 2115–2123.

Burright, E.N., Clark, H.B., Servadio, A., Matilla, T., Feddersen, R.M., Yunis, W.S., Duvick, L.A., Zoghbi, H.Y., and Orr, H.T. (1995). SCA1 transgenic mice: a model for neurodegeneration caused by an expanded CAG trinucleotide repeat. Cell *82*, 937–948.

Cattaneo, E., Zuccato, C., and Tartari, M. (2005). Normal huntingtin function: an alternative approach to Huntington's disease. Nat. Rev. Neurosci. *6*, 919–930.

Chen, H.K., Fernandez-Funez, P., Acevedo, S.F., Lam, Y.C., Kaytor, M.D., Fernandez, M.H., Aitken, A., Skoulakis, E.M., Orr, H.T., Botas, J., et al. (2003). Interaction of Akt-phosphorylated ataxin-1 with 14-3-3 mediates neurodegeneration in spinocerebellar ataxia type 1. Cell *113*, 457–468.

Chen, S., Peng, G.H., Wang, X., Smith, A.C., Grote, S.K., Sopher, B.L., and La Spada, A.R. (2004). Interference of Crx-dependent transcription by ataxin-7 involves interaction between the glutamine regions and requires the ataxin-7 carboxy-terminal region for nuclear localization. Hum. Mol. Genet. *13*, 53–67.

Chen-Plotkin, A.S., Sadri-Vakili, G., Yohrling, G.J., Braveman, M.W., Benn, C.L., Glajch, K.E., DiRocco, D.P., Farrell, L.A., Krainc, D., Gines, S., et al. (2006). Decreased association of the transcription factor Sp1 with genes downregulated in Huntington's disease. Neurobiol. Dis. *22*, 233–241.

Chevalier-Larsen, E.S., O'Brien, C.J., Wang, H., Jenkins, S.C., Holder, L., Lieberman, A.P., and Merry, D.E. (2004). Castration restores function and neurofilament alterations of aged symptomatic males in

a transgenic mouse model of spinal and bulbar muscular atrophy. J. Neurosci. *24*, 4778–4786.

de Chiara, C., Menon, R.P., Dal Piaz, F., Calder, L., and Pastore, A. (2005). Polyglutamine is not all: the functional role of the AXH domain in the ataxin-1 protein. J. Mol. Biol. *354*, 883–893.

Doss-Pepe, E.W., Stenroos, E.S., Johnson, W.G., and Madura, K. (2003). Ataxin-3 interactions with rad23 and valosin-containing protein and its associations with ubiquitin chains and the proteasome are consistent with a role in ubiquitin-mediated proteolysis. Mol. Cell. Biol. *23*, 6469–6483.

Dunah, A.W., Jeong, H., Griffin, A., Kim, Y.M., Standaert, D.G., Hersch, S.M., Mouradian, M.M., Young, A.B., Tanese, N., and Krainc, D. (2002). Sp1 and TAFII130 transcriptional activity disrupted in early Huntington's disease. Science *296*, 2238–2243.

Duyao, M.P., Auerbach, A.B., Ryan, A., Persichetti, F., Barnes, G.T., McNeil, S.M., Ge, P., Vonsattel, J.P., Gusella, J.F., Joyner, A.L., et al. (1995). Inactivation of the mouse Huntington's disease gene homolog Hdh. Science *269*, 407–410.

Emamian, E.S., Kaytor, M.D., Duvick, L.A., Zu, T., Tousey, S.K., Zoghbi, H.Y., Clark, H.B., and Orr, H.T. (2003). Serine 776 of ataxin-1 is critical for polyglutamine-induced disease in SCA1 transgenic mice. Neuron *38*, 375–387.

Eriksen, J.L., Przedborski, S., and Petrucelli, L. (2005). Gene dosage and pathogenesis of Parkinson's disease. Trends Mol. Med. *11*, 91–96.

Fernandez-Funez, P., Nino-Rosales, M.L., de Gouyon, B., She, W.C., Luchak, J.M., Martinez, P., Turiegano, E., Benito, J., Capovilla, M., Skinner, P.J., et al. (2000). Identification of genes that modify ataxin-1-induced neurodegeneration. Nature *408*, 101–106.

Gatchel, J.R., and Zoghbi, H.Y. (2005). Diseases of unstable repeat expansion: mechanisms and common principles. Nat. Rev. Genet. *6*, 743–755.

Gauthier, L.R., Charrin, B.C., Borrell-Pages, M., Dompierre, J.P., Rangone, H., Cordelieres, F.P., De Mey, J., MacDonald, M.E., Lessmann, V., Humbert, S., et al. (2004). Huntingtin controls neurotrophic support and survival of neurons by enhancing BDNF vesicular transport along microtubules. Cell *118*, 127–138.

Graham, R.K., Deng, Y., Slow, E.J., Haigh, B., Bissada, N., Lu, G., Pearson, J., Shehadeh, J., Bertram, L., Murphy, Z., et al. (2006). Cleavage at the caspase-6 site is required for neuronal dysfunction and degeneration due to mutant huntingtin. Cell *125*, 1179–1191.

Harjes, P., and Wanker, E.E. (2003). The hunt for huntingtin function: interaction partners tell many different stories. Trends Biochem. Sci. *28*, 425–433.

Helmlinger, D., Hardy, S., Abou-Sleymane, G., Eberlin, A., Bowman, A.B., Gansmuller, A., Picaud, S., Zoghbi, H.Y., Trottier, Y., Tora, L., et al. (2006). Glutamine-expanded ataxin-7 alters TFTC/STAGA recruitment and chromatin structure leading to photoreceptor dysfunction. PLoS Biol. *4*, e67.

Ikeda, Y., Aihara, K., Sato, T., Akaike, M., Yoshizumi, M., Suzaki, Y., Izawa, Y., Fujimura, M., Hashizume, S., Kato, M., et al. (2005). Androgen receptor gene knockout male mice exhibit impaired cardiac growth and exacerbation of angiotensin II-induced cardiac fibrosis. J. Biol. Chem. *280*, 29661–29666.

Jimenez, G., Guichet, A., Ephrussi, A., and Casanova, J. (2000). Relief of gene repression by torso RTK signaling: role of capicua in Drosophila terminal and dorsoventral patterning. Genes Dev. *14*, 224–231.

Katsuno, M., Adachi, H., Kume, A., Li, M., Nakagomi, Y., Niwa, H., Sang, C., Kobayashi, Y., Doyu, M., and Sobue, G. (2002). Testosterone reduction prevents phenotypic expression in a transgenic mouse model of spinal and bulbar muscular atrophy. Neuron *35*, 843–854.

Kawamura-Saito, M., Yamazaki, Y., Kaneko, K., Kawaguchi, N., Kanda, H., Mukai, H., Gotoh, T., Motoi, T., Fukayama, M., Aburatani, H., et al. (2006). Fusion between CIC and DUX4 up-regulates PEA3 family genes in Ewing-like sarcomas with t(4;19)(q35;q13) translocation. Hum. Mol. Genet. *15*, 2125–2137.

Kegel, K.B., Meloni, A.R., Yi, Y., Kim, Y.J., Doyle, E., Cuiffo, B.G., Sapp, E., Wang, Y., Qin, Z.H., Chen, J.D., et al. (2002). Huntingtin is present in the nucleus, interacts with the transcriptional corepressor C-terminal binding protein, and represses transcription. J. Biol. Chem. *277*, 7466–7476.

Li, S.H., and Li, X.J. (2004). Huntingtin-protein interactions and the pathogenesis of Huntington's disease. Trends Genet. *20*, 146–154.

Li, S.H., Cheng, A.L., Zhou, H., Lam, S., Rao, M., Li, H., and Li, X.J. (2002). Interaction of Huntington disease protein with transcriptional activator Sp1. Mol. Cell. Biol. *22*, 1277–1287.

Lim, J., Hao, T., Shaw, C., Patel, A.J., Szabo, G., Rual, J.F., Fisk, C.J., Li, N., Smolyar, A., Hill, D.E., et al. (2006). A protein-protein interaction network for human inherited ataxias and disorders of Purkinje cell degeneration. Cell *125*, 801–814.

Luo, S., Vacher, C., Davies, J.E., and Rubinsztein, D.C. (2005). Cdk5 phosphorylation of huntingtin reduces its cleavage by caspases: implications for mutant huntingtin toxicity. J. Cell Biol. *169*, 647–656.

MacDonald, M.E. (2003). Huntingtin: alive and well and working in middle management. Sci. STKE *207*, pe48.

Matilla, A., Roberson, E.D., Banfi, S., Morales, J., Armstrong, D.L., Burright, E.N., Orr, H.T., Sweatt, J.D., Zoghbi, H.Y., and Matzuk, M.M. (1998). Mice lacking ataxin-1 display learning deficits and decreased hippocampal paired-pulse facilitation. J. Neurosci. *18*, 5508–5516.

Matsumoto, T., Takeyama, K., Sato, T., and Kato, S. (2005). Study of androgen receptor functions by genetic models. J. Biochem. (Tokyo) *138*, 105–110.

McMahon, S.J., Pray-Grant, M.G., Schieltz, D., Yates, J.R., 3rd, and Grant, P.A. (2005). Polyglutamine-expanded spinocerebellar ataxia-7 protein disrupts normal SAGA and SLIK histone acetyltransferase activity. Proc. Natl. Acad. Sci. USA *102*, 8478–8482.

McManamny, P., Chy, H.S., Finkelstein, D.I., Craythorn, R.G., Crack, P.J., Kola, I., Cheema, S.S., Horne, M.K., Wreford, N.G., O'Bryan, M.K., et al. (2002). A mouse model of spinal and bulbar muscular atrophy. Hum. Mol. Genet. *11*, 2103–2111.

Nasir, J., Floresco, S.B., O'Kusky, J.R., Diewert, V.M., Richman, J.M., Zeisler, J., Borowski, A., Marth, J.D., Phillips, A.G., and Hayden, M.R. (1995). Targeted disruption of the Huntington's disease gene results in embryonic lethality and behavioral and morphological changes in heterozygotes. Cell *81*, 811–823.

Okazawa, H., Rich, T., Chang, A., Lin, X., Waragai, M., Kajikawa, M., Enokido, Y., Komuro, A., Kato, S., Shibata, M., et al. (2002). Interaction between mutant ataxin-1 and PQBP-1 affects transcription and cell death. Neuron *34*, 701–713.

Palhan, V.B., Chen, S., Peng, G.H., Tjernberg, A., Gamper, A.M., Fan, Y., Chait, B.T., La Spada, A.R., and Roeder, R.G. (2005). Polyglutamine-expanded ataxin-7 inhibits STAGA histone acetyltransferase activity to produce retinal degeneration. Proc. Natl. Acad. Sci. USA *102*, 8472–8477.

Pardo, R., Colin, E., Regulier, E., Aebischer, P., Deglon, N., Humbert, S., and Saudou, F. (2006). Inhibition of calcineurin by FK506 protects against polyglutamine-huntingtin toxicity through an increase of huntingtin phosphorylation at S421. J. Neurosci. *26*, 1635–1645.

Rangone, H., Poizat, G., Troncoso, J., Ross, C.A., MacDonald, M.E., Saudou, F., and Humbert, S. (2004). The serum- and glucocorticoid-induced kinase SGK inhibits mutant huntingtin-induced toxicity by phosphorylating serine 421 of huntingtin. Eur. J. Neurosci. *19*, 273–279.

Rigaut, G., Shevchenko, A., Rutz, B., Wilm, M., Mann, M., and Seraphin, B. (1999). A generic protein purification method for protein

complex characterization and proteome exploration. Nat. Biotechnol. *17*, 1030–1032.

Roch, F., Jimenez, G., and Casanova, J. (2002). EGFR signalling inhibits Capicua-dependent repression during specification of Drosophila wing veins. Development *129*, 993–1002.

Ross, C.A., and Poirier, M.A. (2004). Protein aggregation and neurodegenerative disease. Nat. Med. *10* (*Suppl*), S10–S17.

Rovelet-Lecrux, A., Hannequin, D., Raux, G., Le Meur, N., Laquerriere, A., Vital, A., Dumanchin, C., Feuillette, S., Brice, A., Vercelletto, M., et al. (2006). APP locus duplication causes autosomal dominant early-onset Alzheimer disease with cerebral amyloid angiopathy. Nat. Genet. *38*, 24–26.

Schaffar, G., Breuer, P., Boteva, R., Behrends, C., Tzvetkov, N., Strippel, N., Sakahira, H., Siegers, K., Hayer-Hartl, M., and Hartl, F.U. (2004). Cellular toxicity of polyglutamine expansion proteins: mechanism of transcription factor deactivation. Mol. Cell *15*, 95–105.

Steffan, J.S., Agrawal, N., Pallos, J., Rockabrand, E., Trotman, L.C., Slepko, N., Illes, K., Lukacsovich, T., Zhu, Y.Z., Cattaneo, E., et al. (2004). SUMO modification of Huntingtin and Huntington's disease pathology. Science *304*, 100–104.

Strom, A.L., Forsgren, L., and Holmberg, M. (2005). A role for both wild-type and expanded ataxin-7 in transcriptional regulation. Neurobiol. Dis. *20*, 646–655.

Tsai, C.C., Kao, H.Y., Mitzutani, A., Banayo, E., Rajan, H., McKeown, M., and Evans, R.M. (2004). Ataxin *1*, a SCA1 neurodegenerative disorder protein, is functionally linked to the silencing mediator of retinoid and thyroid hormone receptors. Proc. Natl. Acad. Sci. USA *101*, 4047–4052.

Tsuda, H., Jafar-Nejad, H., Patel, A.J., Sun, Y., Chen, H.K., Rose, M.F., Venken, K.J., Botas, J., Orr, H.T., Bellen, H.J., et al. (2005). The AXH domain of Ataxin-1 mediates neurodegeneration through its interaction with Gfi-1/Senseless proteins. Cell *122*, 633–644.

Van Raamsdonk, J.M., Pearson, J., Rogers, D.A., Bissada, N., Vogl, A.W., Hayden, M.R., and Leavitt, B.R. (2005). Loss of wild-type huntingtin influences motor dysfunction and survival in the YAC128 mouse model of Huntington disease. Hum. Mol. Genet. *14*, 1379–1392.

Warby, S.C., Chan, E.Y., Metzler, M., Gan, L., Singaraja, R.R., Crocker, S.F., Robertson, H.A., and Hayden, M.R. (2005). Huntingtin phosphorylation on serine 421 is significantly reduced in the striatum and by polyglutamine expansion in vivo. Hum. Mol. Genet. *14*, 1569–1577.

Warrick, J.M., Morabito, L.M., Bilen, J., Gordesky-Gold, B., Faust, L.Z., Paulson, H.L., and Bonini, N.M. (2005). Ataxin-3 suppresses polyglutamine neurodegeneration in Drosophila by a ubiquitin-associated mechanism. Mol. Cell *18*, 37–48.

Watase, K., Weeber, E.J., Xu, B., Antalffy, B., Yuva-Paylor, L., Hashimoto, K., Kano, M., Atkinson, R., Sun, Y., Armstrong, D.L., et al. (2002). A long CAG repeat in the mouse Sca1 locus replicates SCA1 features and reveals the impact of protein solubility on selective neurodegeneration. Neuron *34*, 905–919.

Yeh, E., Gustafson, K., and Boulianne, G.L. (1995). Green fluorescent protein as a vital marker and reporter of gene expression in Drosophila. Proc. Natl. Acad. Sci. USA *92*, 7036–7040.

Zeitlin, S., Liu, J.P., Chapman, D.L., Papaioannou, V.E., and Efstratiadis, A. (1995). Increased apoptosis and early embryonic lethality in mice nullizygous for the Huntington's disease gene homologue. Nat. Genet. *11*, 155–163.

Zhai, W., Jeong, H., Cui, L., Krainc, D., and Tjian, R. (2005). In vitro analysis of huntingtin-mediated transcriptional repression reveals multiple transcription factor targets. Cell *123*, 1241–1253.

Zuccato, C., Tartari, M., Crotti, A., Goffredo, D., Valenza, M., Conti, L., Cataudella, T., Leavitt, B.R., Hayden, M.R., Timmusk, T., et al. (2003). Huntingtin interacts with REST/NRSF to modulate the transcription of NRSE-controlled neuronal genes. Nat. Genet. *35*, 76–83.